Acta Astronautica 137 (2017) 444–449

Contents lists available at ScienceDirect

Acta Astronautica

journal homepage: www.elsevier.com/locate/actaastro

# Experimental investigation on the impacts of ignition energy and position on ignition processes in supersonic flows by laser induced plasma

Bin An*, Zhenguo Wang, Leichao Yang, Xipeng Li, Jiajian Zhu

*Science and Technology on Scramjet Laboratory, College of Aerospace Science and Engineering, National University of Defense Technology, Changsha, Hunan 410073, China*

ARTICLE INFO

*Keywords:*
Ignition
Supersonic flows
Laser
Plasma

ABSTRACT

Cavity ignition of a model scramjet combustor fueled by ethylene was achieved through laser induced plasma, with inflow conditions of $Ma = 2.92$, total temperature $T_0 = 1650$ K and stagnation pressure $P_0 = 2.6$ MPa. The overall equivalent ratio was kept at 0.152 for all the tests. The ignition processes at different ignition energies and various ignition positions were captured by $CH^*$ and $OH^*$ chemiluminescence imaging. The results reveal that the initial flame kernel is carried to the cavity leading edge by the recirculation flow, and resides there for ~100 μs before spreading downstream. The ignition time can be reduced, and the possibility of successful ignition for single laser pulse can be promoted by enhancing ignition energy. The scale and strength of the initial flame kernel is influenced by both the ignition energy and position. In present study, the middle part of the cavity is the best position for ignition, as it keeps a good balance between the strength of initial flame kernel and the impacts of strain rate in recirculation flow.

## 1. Introduction

Successfully igniting scramjet combustors is a challenging work because of the conflict between the limited residence times and comparatively longer ignition delay times of hydrocarbon fuels [1,2]. Besides, the inhomogeneous fuel-air mixing and high strain rate in supersonic flows make the task even harder [3,4]. For the purpose of achieving reliable ignition, various methods have been proposed. Dual-cavity scheme was employed by Li et al. [4] to enhance the ignition ability of a scramjet combustor fueled by kerosene. Ombrello et al. [5] applied spark discharge and pulse detonator to ignite an ethylene fueled cavity at Mach 4 flight condition. The experimental results of Do et al. [6] indicted that the nonequilibrium plasma produced by pulsed discharged electrodes reduced the ignition delay times of both $H_2$-air mixture and ethylene-air mixture. Sun et al. [7] investigated the spark ignition process in a combustor equipped with multi-cavities with an isolator entrance Mach number of 1.92. Other techniques such as plasma torches [8], pilot hydrogen [9] and mechanical throttle [10] were proved to have positive effect on ignition too.

As an advanced ignition method, laser induced plasma ignition (LIPI) has been developed for decades in the field of internal combustion engines [11,12]. Massive fundamental research work which was done in quiescent gases and low-speed air-fuel mixtures [13,14] suggested that LIPI might be a promising ignition technique for future engines. However, investigation on LIPI in supersonic airstreams is exiguous. Horisawa et al. [15] numerically studied the effects of laser induced plasma for combustion and mixing enhancements in a constant area combustor. The formation of flame kernel and propagation of shockwave induced by plasma were well captured. According to the distributions of OH radical, the flame moved upstream first and then downstream from the ignition point because of the recirculation zones induced by shockwave and hydrogen jet. Brieschenk et al. [16–18] experimentally investigated the behavior of LIPI in hypersonic flows. A Q-switched laser with pulse energy of 750 mJ was used to ignite hydrogen in the experiment. The hydroxyl radical fluorescence induced by planer laser was captured for combustion visualization. As no flame-holder was applied, the flame extinguished in less than 100 μs. Yang et al. [19–21] succeeded in igniting ethylene and kerosene in supersonic flows through laser induced plasma.

Although the ignition processes of LIPI in supersonic flows have been revealed in previous work, more delicate research should be done for in-depth understanding of the mechanism. In the present work, a Q-switched Nd: YAG laser is utilized for igniting a model scramjet combustor. The flame structure and propagation are captured spatially and temporally by recording $CH^*$ and $OH^*$ chemiluminescence simultaneously. The differences of ignition processes at various ignition energies

* Corresponding author.
*E-mail address:* anbinsky@163.com (B. An).

http://dx.doi.org/10.1016/j.actaastro.2017.05.013
Received 22 January 2017; Accepted 15 May 2017
Available online 17 May 2017

and ignition positions are compared in detail.

## 2. Experimental description

A direct-connected test facility which was composed of an air heater, a supersonic nozzle and a scramjet model combustor was used for the experiments. By burning pure ethanol and oxygen, the air heater was capable of continuously heating air from atmosphere condition to where stagnation temperature $T_0 = 1650$ K, total pressure $P_0 = 2.6$ MPa at a mass flow rate of 1 kg/s. The mole fraction of oxygen in the vitiated air was 21%. The outlet of air heater was equipped with a two-dimensional Larval-nozzle to accelerate heated air to $Ma = 2.92$.

Shown in Fig. 1 is the model scramjet engine. A constant-area 315 mm long isolator with height of 40 mm and width of 50 mm is directly connected to the exit of nozzle, followed by a 512-mm-long combustor whose lower wall diverges at an angle of 2.25°. A 220 mm long expansion section with a single-side expansion angle of 3° is at the end of the combustor. One cavity is installed on the lower wall.

As illustrated in Fig. 2, the cavity depth $D = 15$ mm, cavity length to depth ratio $L/D = 7$, and the aft ramp angle is 45°. Ethylene at room temperature was injected through a 2-mm-diam orifice which is located at 10 mm upstream to the cavity leading edge and in the middle in span wise. The pressure of ethylene before being injected was 2.5 MPa. The overall equivalent ratio was kept at 0.152 for all the tests. A Q-switched Nd: YAG laser system (Vlite-500) was used for ignition. The laser system could provide 532 nm laser pulse with width of 10 ns, diameter of 12 mm and maximum energy of 350 mJ. But, only 85% of the laser pulse energy passed through the lens and the quartz window of the combustor. The laser pulses were focused by a convex lens ($f = 150$ mm) to produce plasma for ignition. The breakdown region that is denoted by red spot in Fig. 2 is in the shape of cone with 3.5 mm in diameter and 5.2 mm long when the output energy of the laser is approximately 300 mJ. Three ignition positions which are in the symmetry plane of the combustor are selected for present study. All of them are in the cavity, and are 5 mm above the bottom of the cavity. From upstream to downstream, their distances to the fore wall of the cavity are 22.5 mm, 45.0 mm and 67.5 mm respectively. For brevity, they are denoted as "P1", "P2" and "P3" separately.

For the purpose of marking flame location clearly, both $CH^*$ and $OH^*$ chemiluminescence were captured simultaneously. $CH^*$ chemiluminescence was recorded by a high-speed camera (Photron SA-Z) with a Nikon 85 mm f/1.8 lens and a bandpass filter (centered at 430 nm, with a 10 nm FWHM). The frame rate of the camera was set at 25,000 frames per second (fps) with an exposure time of 40 μs. An intensified charge-coupled device (ICCD) camera equipped with a UV lens (95 mm focal length and f/4.1) and a bandpass filter (centered at 311 nm, with a 10 nm FWHM) was applied to acquire $OH^*$ chemiluminescence. The ICCD camera operated at 3 fps with a shutter time of 2 μs. The spatial resolution of the high-speed camera and ICCD camera were 240 μm per pixel and 250 μm per pixel respectively. As the cameras were mounted on the same side, neither of them oriented normal to test section precisely. The consequent image distortion was corrected by data processing program. What's more, with the help of two Digital Delay/Pulse Generators (DG535), the operation time of the ignition laser system and two cameras could be controlled accurately.

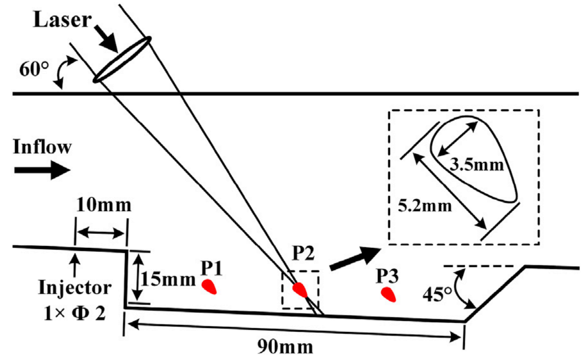


**Fig. 2.** Schematic of cavity and optics.

## 3. Results and discussion

### 3.1. The effects of ignition energy on ignition processes

The impacts of ignition energy on ignition behaviors were studied with ignition position at P2. A representative set of $CH^*$ chemiluminescence images are shown in Fig. 3 with ignition energies $E_1 = 303.6 \pm 7.4$ mJ and $E_2 = 230.7 \pm 6.0$ mJ. The intensity of each pixel is normalized by the maximum intensity of all the pixels during ignition processes. In order to provide good contrast these images are displayed in false-color.

As shown in Fig. 3, for the ignition energy $E_1$, the flame kernel at 40 μs is bright and located in the middle of cavity. By 120 μs the flame kernel has moved to the cavity leading edge, following the recirculation zone, but has become smaller and less bright. After being anchored there, it grows slightly in strength from 120 μs to 200 μs. Then it begins propagating to the downstream at 200 μs, and has filled the cavity by 560 μs. Later in time, the flame kernel spreads into the mainstream from the aft wall in 80 μs. At last, the combustor settles into a quasi-stable burning process by 720 μs.

By contrast, when the ignition energy is reduced to $E_1$ the initial flame kernel is smaller. It takes 1120 μs for the flame kernel to fulfill the cavity and propagate to the mainstream, which is 400 μs longer than the ignition process of $E_1$. It is also noteworthy that the flame kernel is suppressed in the cavity during most time of the ignition process, for the high speed flow and consequent high strain rate in the mainstream. Besides, the flame intensity in the shear layer is much stronger than its counterpart elsewhere when the flame kernel spreads from the cavity leading edge to aft wall. Because the shear layer is rich in air-ethylene mixture.

In order to go beyond qualitative images, the total $CH^*$ chemiluminescence intensity from the observation area which is shown in Fig. 3 versus time is displayed in Fig. 4. The total chemiluminescence intensity is normalized by time averaged total chemiluminescence intensity when the combustor is at stable combustion condition. In an attempt to minimize the impacts of random elements involved, data from eight tests are used to plot one curve.

As presented in Fig. 4, the ignition processes can be divided into five stages according to the normalized intensity which is correspond to heat release. Take the curve with ignition energy $E_1 = 303.6$ mJ for example, the normalized intensity decreases sharply in stage I which lasts for approximately 120 μs after laser pulse. During this period the normalized

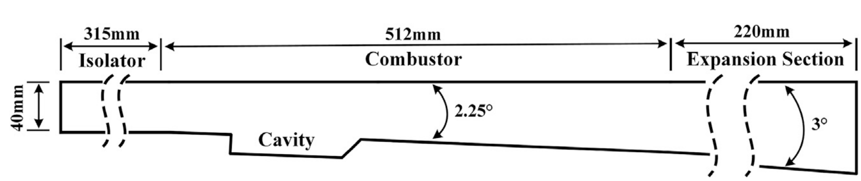


**Fig. 1.** Schematic of the model scramjet engine and cavity installation.